CONF-900936--7

MICROSTRUCTURES OF CUBIC Al_2O_3 PRECIPITATES IN OXYGEN-IMPLANTED ALUMINUM

D. M. Follstaedt, S. M. Myers and R. J. Bourcier

Sandia National Laboratories

Albuquerque, NM 87185-5800 USA

SAND--90-0993C

DE91 000038

ABSTRACT

The microstructure of Al ion-implanted at room temperature with 17 at.% O has been characterized with TEM. The alloy has extremely small (1.5 - 3.5 nm) oxide precipitates whose crystal structure is interpreted to be a disordered version of γ-Al_2O_3 having a fcc lattice of O^{2-} ions with Al^{3+} ions in random interstitial sites. The small sizes can account for the exceptionally high strength of as-implanted alloys: 2500 - 3300 MPa. Larger precipitates are found when the alloy is annealed 1/2 hour at 550°C, which is consistent with its somewhat lower strength: 800 - 1600 MPa.

1. Introduction

Ion implantation into metals [1] can form near-surface alloys with solute concentrations far above equilibrium solubilities. The phases of the implanted layers are frequently metastable. If kinetics permit precipitation to occur, the particles are usually small and dense in number. These novel microstructures can produce alloy layers with superior mechanical properties. All these special features are found in Al implanted with O.

Previously, nanoindentation of Al implanted with 5, 10 or 20 at.% O and annealed at 550°C showed it to be much harder than pure Al [2]. Furthermore, finite-element mechanical modeling of the indentation indicated that the implanted layer has a very high flow stress: 800 - 1600 MPa, for 20 at.% O. This alloy contained a high density of small γ-Al_2O_3 precipitates 4 - 10 nm in diameter. Conventional precipitation hardening theories applied to this very refined microstructure quantitatively account for the high strength [2].

More recently, as-implanted Al alloys with 20 at.% O have been found to have an even higher flow stress of 2500 - 3300 MPa [3]. The strengths of the implanted alloy layers are seen to be exceptionally high when compared to the Al alloys listed in Fig. 1. Pure Al has a very low yield stress of 40 MPa, while even that of 7075-T6, a high-strength aerospace Al alloy, is only 500 MPa. The strength of the as-implanted alloy even exceeds that of hardened 440C bearing steel.

Here we characterize the as-implanted microstructure and compare it with that after annealing at 550°C. The as-implanted alloy has very small oxide precipitates (1.5 - 3.5 nm in diameter) which are a disordered version of the γ-Al_2O_3 phase found after annealing. The smaller sizes can quantitatively account for the increased strength of the as-implanted alloy.

A pure Al foil with large grains (>~100 μm) was implanted with 1.5×10^{17} O/cm^2 at 50 keV, followed by 5.7×10^{16} O/cm^2 at 25 keV. The foils

were clamped to the specimen holder, and implantation was done with currents $\leq 2.7\ \mu A/cm^2$. This sequence was calculated to produce a near-surface alloy with a concentration of 20 at.% O. Rutherford backscattering 2.0 MeV ^4He indicated a slightly smaller value, 17±1 at.% O, which extended to a depth of 0.11 μm. This concentration greatly exceeds the vanishingly small solid solubility of O in Al (<$3x10^{-8}$ at.% [4]). Disks were punched from the foil and back-thinned by jet electropolishing for transmission electron microscopy (TEM) examination, or were annealed 1/2 hour at 550°C and then examined.

2. **Microstructure of Annealed Alloys**

It is useful to discuss the annealed alloy first, since the crystal structure of its precipitates is clearly identified. Bright-field images show very mottled Al diffraction contours with small white areas (~10 nm), which suggest that a second phase is present. Electron diffraction patterns have additional, less intense reflections midway between those of fcc Al, as shown in Fig. 2a) for a <100> zone axis. Tilting off the axis reduces the intensity of the Al reflections and allows other oxide reflections to be resolved beside them at a slightly larger radial distance; the two spots are seen in the enlarged (3x) insert of Fig. 2b). Other patterns show reflections elongated in <111> directions, which suggests that the particles are thinner in these directions. All the additional reflections are accounted for by identifying the precipitates as γ-Al_2O_3 and aligning its cubic axes with those of the fcc matrix. This metastable phase has been previously identified in O-implanted Al [5,6].

Two sets of precipitates are identified by using two different imaging methods. First, bright-field imaging in weakly diffracting areas (away from Al diffraction contours) shows a high areal fraction of particles, whose contrast can be enhanced by imaging slightly out of focus. Figure 2c) shows an underfocussed condition with a white edge appears around the particles;

the edge becomes dark in overfocus. This contrast variation is opposite to that of cavities, and implies that there is stronger electron scattering in particle areas than in matrix areas of the specimen. The stronger scattering could be due to surface relief associated with the particles, implying that they are close to the surface. However, some particles appear to overlap each other, and particle number is reduced in thinner specimen areas; these two features suggest that the particles are distributed in depth. The stronger scattering might then be due to the higher total-atom density of Al_2O_3 (1.082×10^{23} at./cm^3) relative to fcc Al (0.602×10^{23} at./cm^3). Thus the depth of these 10 - 25 nm particles in the implanted layer is not clear.

The second method, dark-field imaging, illuminates both sets of precipitates. Imaging can be done with either the γ-phase ordering reflections located between the intense reflections of fcc Al or the stronger reflections adjacent to those of Al when the sample is tilted off axis. An image taken with the adjacent reflection indicated in Fig. 2b) is shown in Fig. 2d). The matrix image illuminated with the Al reflection is weaker than that of the oxide particles seen in this area. A few large, bright particles (up to 25 nm) apparently belonging to the first set are readily seen; their number is reduced from that in Fig. 2c) because of the tilting. However, close examination also shows a dense distribution of less-intense, smaller particles. The second set of smaller particles seen in this and other dark-field images are 2 - 8 nm. The ranges of size make it hard to distinguish the two particle sets and imaging the second set is difficult in dark field, but a high density of particles as small as ~2 nm can be identified.

Thus the annealed alloy contains γ-Al_2O_3 precipitates with a broad, bimodal distribution of sizes, 2 - 25 nm, which includes that previously reported for 20 at.% Al (4 - 10 nm). Proximity to the surface may have influenced the large precipitates. The γ-Al_2O_3 structure [7] consists of a

fcc sublattice of O^{2-} ions with Al^{3+} ions in interstitial sites. The Al^{3+} ions occupy an ordered set of (111) planes, and this ordering doubles the fcc cell size to produce a cubic cell with a_o = 0.790 nm. This value is only 2.5% less than twice that of Al ($2a_o$ = 0.8098 nm), which gives a high degree of coherency between the matrix and the small oxide particles, as discussed previously [6]. The ordering and doubled cell size produce the isolated reflections seen between those of Al.

3. **Microstructure of As-Implanted Alloys**

Oxide precipitates are also present in the as-implanted alloy, but do not produce readily observed reflections in any zone-axis diffraction patterns, such as the <100> pattern in Fig. 3a) (compare with Fig. 2a)). The absence of the isolated reflection indicates that the oxide is not chemically ordered. However, when the specimen is tilted off an axis, additional diffuse reflections are seen. The pattern in Fig. 3c) was obtained by tilting the specimen ~5° off a <100> zone axis. Weak, diffuse reflections are seen beside the sharp Al reflection of reduced intensity on either side of the bright row; the 3x enlarged insert in Fig. 3c) shows both. A diffuse reflection is seen at the position of each Al reflection when the specimen is appropriately tilted off any axis. No other reflections are observed.

The diffuse spots are due to very small oxide precipitates with an fcc structure. Tilting off axis reduces the Al intensity, but low-intensity relrods in three-dimensional reciprocal space still intersect the Ewald sphere and produce sharp, weak spots in the diffraction pattern, as illustrated schematically in Fig 4. Tilting reduces the oxide intensities to a lesser extent than those of Al because the reflections are very broad in reciprocal space due to the small particle size.

The precipitates are readily detected as small white spots against the dark, strongly diffracting Al matrix in the bright-field image of Fig. 3c).

Larger particles like those in the annealed sample were not found in this alloy. Dark-field imaging allows them to be sized more accurately, and can be done in two ways. A weak-beam image can be obtained by tilting the incident electron beam to shift the strong reflection seen in Fig. 3b) to the central axis; this image is shown in Fig. 3d). Many dislocations which result from lattice displacements during the ion implantation are seen with their cores illuminated, and a high density of the very small oxide particles is seen between them. Secondly, imaging with a diffuse spot and the specimen tilted ~5° off axis as in Fig. 3b) produced Fig. 3e); the Al image illuminated in this area is very weak. Examination of all the images indicates that most of the precipitates in the as-implanted alloy are 1.5 - 3.5 nm in diameter. It is possible that smaller particles are also present but are not detected due to overlap with other particles and instrument resolution (~0.7 nm).

4. Discussion

The smaller precipitate sizes in the as-implanted alloy imply a higher number density than in the annealed alloy, which is consistent with its higher strength. In fact, the observed sizes give quantitative agreement with the flow stress when all the oxygen is presumed to have precipitated and a dispersion strengthening model is used, as discussed elsewhere [3,8]. A second mechanism, coherency strengthening, appears unable to account fully for the strength of the as-implanted alloy, unless the lattice misfit between the disordered precipitates and matrix has increased significantly beyond the 2.5% for ordered γ-Al_2O_3 and fcc Al [3,6].

Several features indicate that the anneal at 550°C produced significant precipitate evolution. The appearance of the ordering reflections indicates Al^{3+} motion within the precipitates. The oxide reflections at the fcc position are significantly sharper in the annealed alloy, which indicates

that the average precipitate size is larger, as confirmed by imaging. The precipitates in the as-implanted alloy (1.5 - 3.5 nm) are not nearly as large as the first set (10 - 25 nm) in the annealed alloy, and even the second, smaller set (2 - 7.5 nm) appears larger than those in the as-implanted alloy.

The authors wish to thank D.M. Bishop for performing the implantations, D.T. Schmale for indentation testing, and M.P. Moran for preparing the TEM specimens. This work was supported by the U.S. Department of Energy under contract no. DE-AC04-76-DP00789.

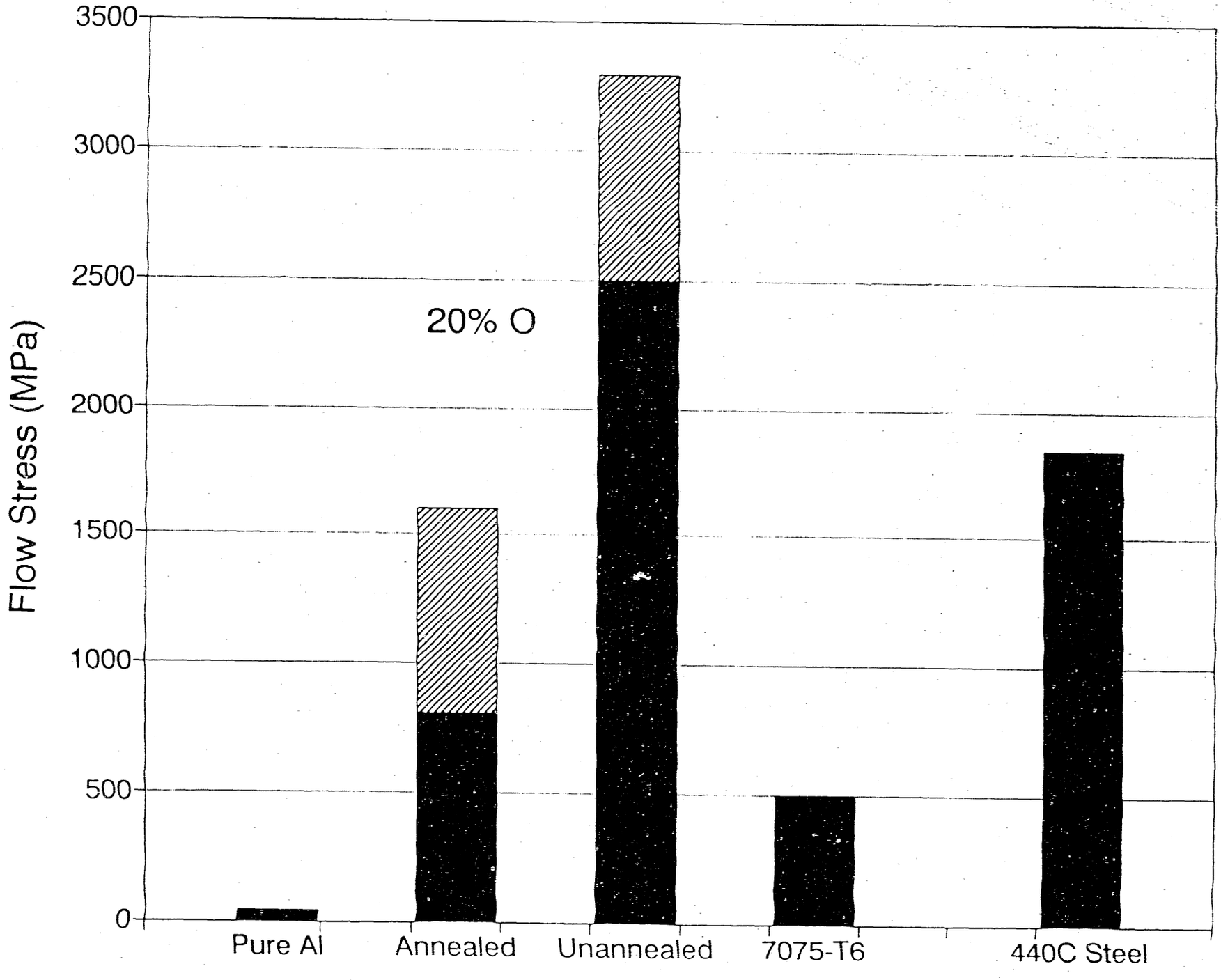
Flow Stress (MPa)
3500
3000
2500
2000
1500
1000
500
0
20% O
Pure Al
Annealed
Unannealed
7075-T6
440C Steel

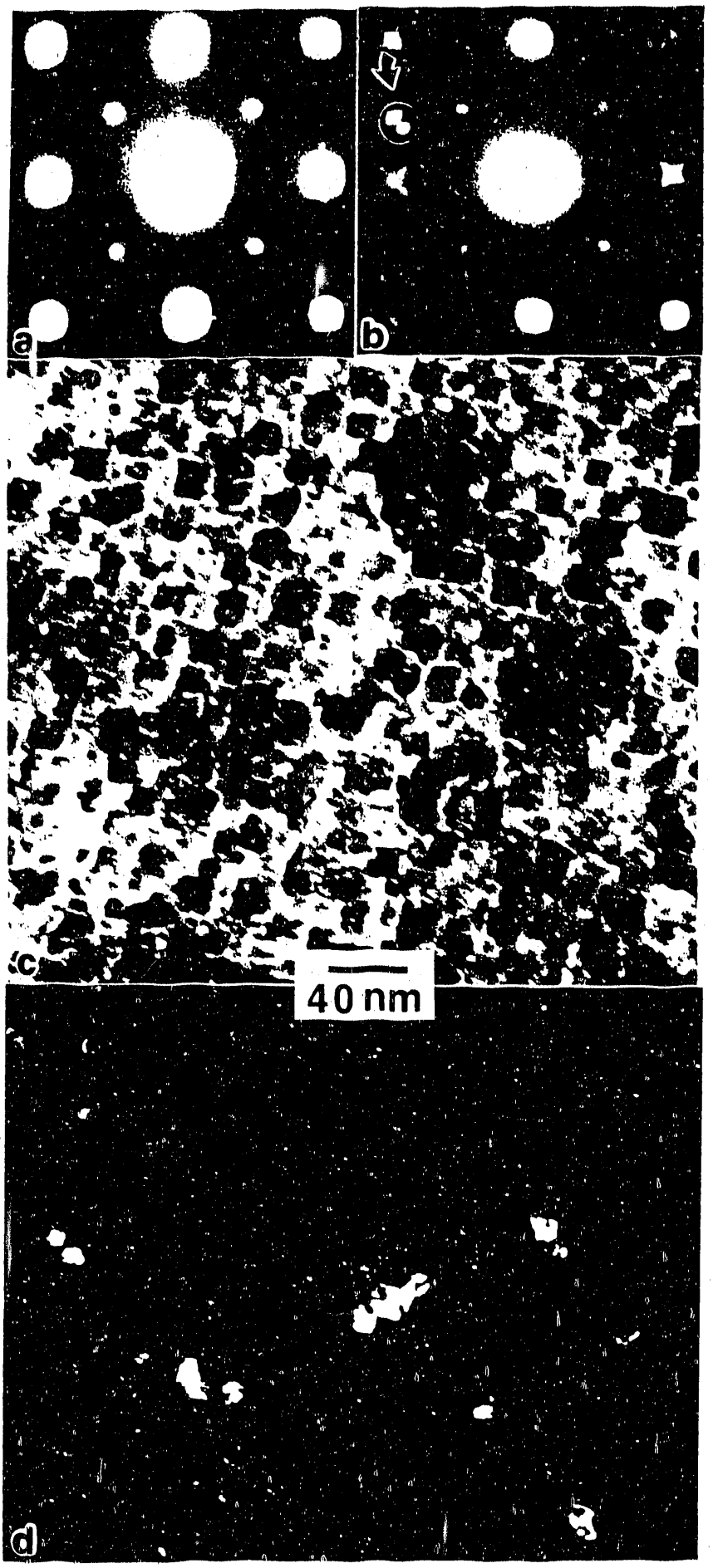
a
b
c
40 nm
d

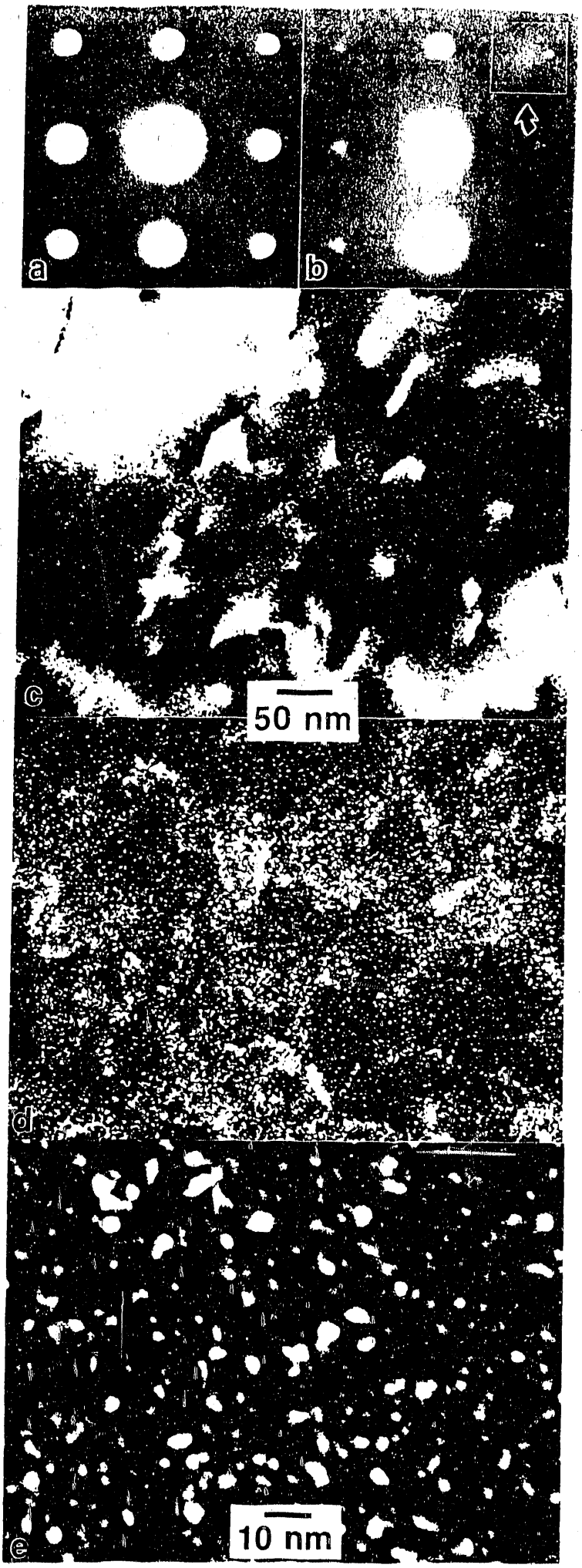
a
b
c
50 nm
d
e
10 nm

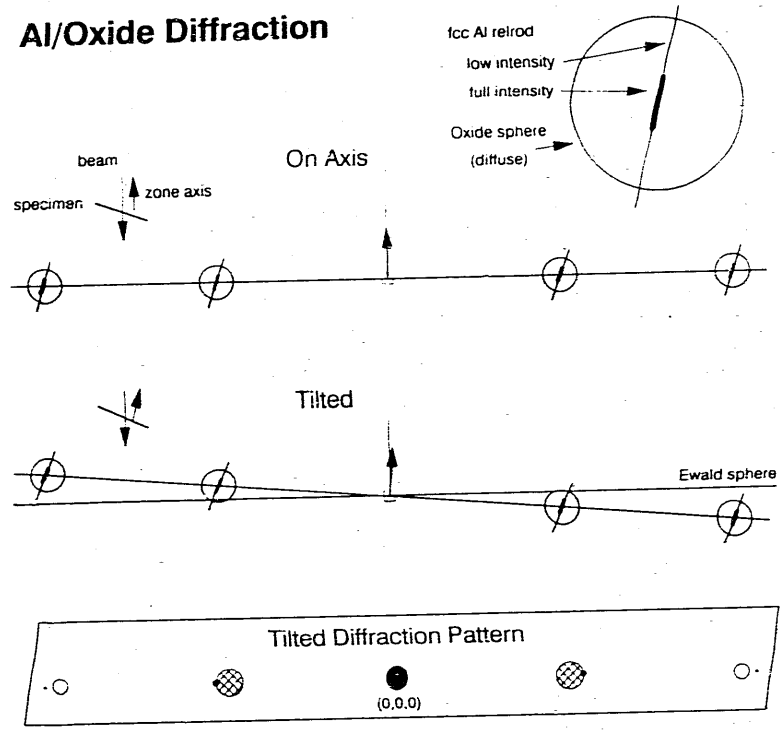
Al/Oxide Diffraction
fcc Al relrod
low intensity
full intensity
Oxide sphere
(diffuse)
On Axis
beam
specimen
zone axis
Tilted
Ewald sphere
Tilted Diffraction Pattern
(0,0,0)

END

DATE FILMED

10/19/90